Reynolds Stress and Eddy Diffusivity of β-Plane Shear Flows

KAUSHIK SRINIVASAN AND W. R. YOUNG

Scripps Institution of Oceanography, University of California, San Diego, La Jolla, California

ABSTRACT

The Reynolds stress induced by anisotropically forcing an unbounded Couette flow, with uniform shear γ, on a β plane, is calculated in conjunction with the eddy diffusivity of a coevolving passive tracer. The flow is damped by linear drag on a time scale μ^{-1}. The stochastic forcing is white noise in time and its spatial anisotropy is controlled by a parameter α that characterizes whether eddies are elongated along the zonal direction ($\alpha < 0$), are elongated along the meridional direction ($\alpha > 0$), or are isotropic ($\alpha = 0$). The Reynolds stress varies linearly with α and nonlinearly and nonmonotonically with γ, but the Reynolds stress is independent of β. For positive values of α, the Reynolds stress displays an "antifrictional" effect (energy is transferred from the eddies to the mean flow); for negative values of α, it displays a frictional effect. When $\gamma/\mu \ll 1$, these transfers can be identified as negative and positive eddy viscosities, respectively. With $\gamma = \beta = 0$, the meridional tracer eddy diffusivity is $\overline{v'^2}/(2\mu)$, where v' is the meridional eddy velocity. In general, nonzero β and γ suppress the eddy diffusivity below $\overline{v'^2}/(2\mu)$. When the shear is strong, the suppression due to γ varies as γ^{-1} while the suppression due to β varies between β^{-1} and β^{-2} depending on whether the shear is strong or weak, respectively.

1. Introduction

In this work we consider a canonical linear problem: the stochastically forced, linearized β-plane vorticity equation with a background mean shear γ:

$$\zeta'_t + \gamma y \zeta'_x + \beta v' + \mu \zeta' = \xi. \qquad (1)$$

The eddy vorticity is related to the eddy streamfunction by $\zeta' = \psi'_{xx} + \psi'_{yy}$, and the eddy velocities are $(u', v') = (-\psi'_y, \psi'_x)$. The random forcing $\xi(x, y, t)$ is spatially homogenous and white noise in time and is characterized more precisely in section 2. Drag, with coefficient μ, is the dissipative mechanism.

Our main concern is the eddy transport of momentum, potential vorticity, and tracer in the ultimate statistically steady state of the model (1). Despite the evident importance of this linear problem, to our knowledge, it has only been discussed previously by Farrell and Ioannou (1993) and Bakas and Ioannou (2013) for the case of weak background shear. The problem is, however, closely related to the initial value problem for the evolution of linearized disturbances on an unbounded viscous Couette flow, first considered by Kelvin (1887) and Orr (1907). A main result of these early studies is that an initial sinusoidal disturbance with crests "leaning" into the shear is amplified for some time. Various aspects of the Kelvin–Orr initial value problem, such as the inclusion of planetary vorticity gradient β and a spectrum of initial disturbances, were subsequently discussed by Rosen (1971), Tung (1983), Boyd (1983), and Shepherd (1985). The transient amplification of Kelvin and Orr is now understood as one consequence of the nonnormality of the linear vorticity equation in the energy norm (Farrell 1982).

In conjunction with the vorticity equation in (1), it is instructive to consider the coevolution of a passive tracer $c'(x, y, t)$ satisfying the linearized tracer equation

$$c'_t + \gamma y c'_x + \beta_c v' + \mu c' = 0, \qquad (2)$$

where β_c is the large-scale tracer gradient. For simplicity, we assume that the scalar damping rate μ is the same as that of the vorticity. The tracer c' differs from the vorticity ζ' because there is no stochastic forcing in (2). Instead, scalar fluctuations are created by the eddy velocity v' stirring the mean gradient β_c.

Corresponding author address: Kaushik Srinivasan, Scripps Institution of Oceanography, University of California, San Diego, Scripps Grad. Dept., 9500 Gilman Dr., La Jolla, CA 92093-0230. E-mail: ksriniva@ucsd.edu

Statistically steady solutions of (1) and (2) are characterized by the Reynolds stress

$$\sigma \stackrel{\text{def}}{=} \overline{u' v'} \qquad (3)$$

and the tracer eddy diffusivity

$$\kappa_e \stackrel{\text{def}}{=} -\frac{\overline{v' c'}}{\beta_c}. \qquad (4)$$

The overbar above indicates either a zonal or an ensemble average. Using the correlation-function formalism of Srinivasan and Young (2012), we provide explicit analytic results for σ, κ_e, and other quadratic statistics, such as the eddy kinetic energy and enstrophy, and the anisotropy of the velocity field.

The correlation function formalism—introduced in sections 2 and 4—is an economical framework for analysis of the statistically steady flow. Rather than solving (1) and (2) explicitly and then averaging the solution, one averages at the outset, and then solves steady deterministic equations that directly provide σ and κ_e.

Farrell and Ioannou (1993) have previously discussed the statistically steady flow corresponding to (1) with $\beta = 0$. Farrell and Ioannou (1993) use the eddy kinetic energy (rather than σ and κ_e) as the main statistical descriptor of the flow and they emphasize viscosity (rather than Ekman drag) as the dissipative mechanism. In a related geophysical context, the tracer equation has recently been considered (with $\gamma = 0$) by Ferrari and Nikurashin (2010) and Klocker et al. (2012).

The forcing and drag terms in (1) incorporate the effects of two different processes, which we characterize as "external" and "internal." External processes, such as small-scale convection in planetary atmospheres (Smith 2004; Scott and Polvani 2007) or baroclinic instability (Williams 1978), are often modeled as a stochastic driving agent combined with a damping term representing Ekman friction. On the other hand, internal nonlinear interactions—that is, $J(\psi', \zeta')$—are sometimes represented using a stochastic turbulence model (DelSole 2001). This is the interpretation of ξ and μ in the studies of Farrell and Ioannou (2003, 2007), Ferrari and Nikurashin (2010), and Klocker et al. (2012). As suggested by fluctuation–dissipation arguments, the turbulence model has a stochastic forcing term and eddy damping; the combination ensures energy conservation. In section 2, we introduce a forcing that is distributed anisotropically around a circle in wavenumber space.

Section 2 contains a description of the forcing structure and symmetries of the correlation functions. Section 3 shows that (1) and (2) have a statistical Galilean symmetry implying that all quadratic statistics, in particular σ and

κ_e, are independent of y. Section 4 summarizes the quadratic power integrals that follow from taking quadratic averages of (1) and (2). These power integrals are used to obtain some simple and general bounds on σ and κ_e. Analytic expressions for σ and κ_e are presented in sections 5 and 6. Section 7 is a conclusion and discussion of the results. Technical details are relegated to the appendixes.

2. Correlation functions and statistical symmetries

We assume that the stochastic forcing $\xi(x, y, t)$ in (1) is temporal white noise, with a two-point, two-time correlation function

$$\overline{\xi(\mathbf{x}_1, t_1)\xi(\mathbf{x}_2, t_2)} = \delta(t_1 - t_2)\Xi(\mathbf{x}). \qquad (5)$$

We restrict attention to spatially homogeneous forcing, so that Ξ depends only on the difference $\mathbf{x} = \mathbf{x}_1 - \mathbf{x}_2$.

We do not assume that the forcing is isotropic: $\Xi(\mathbf{x})$ might depend on the direction of the two-point separation $\mathbf{x} = (x, y)$. One motivation for examining the effect of anisotropy is that in many studies of zonal jets on the β plane (Vallis and Maltrud 1993; Smith 2004) and on the sphere (Williams 1978; Scott and Polvani 2007; Showman 2007), the small-scale forcing used to drive the jets is assumed to be isotropic, even though the physical processes that the forcing models, such as baroclinic instability in the ocean and moist convection in planetary atmospheres, are typically not isotropic (Arbic and Flierl 2004; Li et al. 2006).

a. A remark on scale separation and homogeneity in y

The background mean flow, γy in (1), can be interpreted as a local approximation to a mean flow $U(y)$ that is slowly varying relative to the eddy scale and to the scale of $\Xi(\mathbf{x})$. At a particular position y, the mean flow is

$$U(y) \approx U(0) + \gamma y, \qquad (6)$$

where $\gamma = U'(0)$. However, the constant $U(0)$ has no physical consequences in this model: one can move the origin of the coordinate system with $\tilde{y} = y + U(0)/\gamma$ to remove $U(0)$ from the problem. This removal hinges on the spatial homogeneity of the statistical properties of $\xi(x, y, t) = \xi[x, \tilde{y} - U(0)/\gamma, t]$. In particular, Ξ is unaltered by this shift of the origin.

b. Statistical properties of the solution

The statistical properties of the solution are encapsulated in two-point same-time correlation functions:

$$\mathcal{Z}(\mathbf{x}) \stackrel{\text{def}}{=} \overline{\zeta_1' \zeta_2'}, \quad \text{and} \quad \Psi(\mathbf{x}) \stackrel{\text{def}}{=} \overline{\psi_1' \psi_2'}. \tag{7}$$

In (7), $\zeta_n' = \zeta'(x_n, y_n, t)$ is the eddy vorticity at point (x_1, y_1) and likewise for ψ_n'; x and y are the components of the two-point separation $\mathbf{x} = \mathbf{x}_1 - \mathbf{x}_2$. In (7), we have anticipated that statistical properties of the solution are spatially homogeneous so that the correlation functions $\mathcal{Z}$ and Ψ depend only on the separation $\mathbf{x} = \mathbf{x}_1 - \mathbf{x}_2$. The correlation functions are connected by the biharmonic equation

$$\mathcal{Z} = (\partial_x^2 + \partial_y^2)^2 \Psi. \tag{8}$$

The statistics of the scalar are characterized by

$$P(\mathbf{x}) \stackrel{\text{def}}{=} \overline{\psi_1' c_2'} \quad \text{and} \quad Q(\mathbf{x}) \stackrel{\text{def}}{=} \overline{\psi_2' c_1'} \quad \text{and} \tag{9}$$

$$C(\mathbf{x}) \stackrel{\text{def}}{=} \overline{c_1' c_2'}. \tag{10}$$

c. Exchange symmetries

Because the notation of one point as ''1'' and the other point as ''2'' is arbitrary, the correlation function Ξ has the ''exchange symmetry''

$$\Xi(x, y) = \Xi(-x, -y). \tag{11}$$

The exchange symmetry implies that Ξ is unchanged by a rotation of 180° in the plane of $\mathbf{x}$, and ensures that the spectrum,

$$\tilde{\Xi}(p, q) \stackrel{\text{def}}{=} \iint e^{-ipx - iqy} \Xi(x, y) \, dx \, dy, \tag{12}$$

is real.

The autocorrelations functions $\mathcal{Z}$, Ψ, and C all satisfy the exchange symmetry (11). For the mixed statistics in (9), exchange implies

$$P(x, y) = Q(-x, -y). \tag{13}$$

The Fourier transform of this relation shows that

$$\tilde{P}(p, q) = \tilde{Q}^*(p, q). \tag{14}$$

d. Reflexion symmetry

If the statistics of the forcing are reflexionally symmetric in the axis of x, then the correlation function has a second symmetry

$$\Xi(x, y) = \Xi(x, -y). \tag{15}$$

The exchange symmetry (11) in concert with (15) implies that Ξ is an even function of both arguments.

Now the left-hand side of (1) is unchanged by

$$\psi \to \psi, \quad t \to t, \quad x \to x, \tag{16}$$

$$\gamma \to -\gamma, \quad y \to -y. \tag{17}$$

This transformation induces $(u', v') \to (-u', v')$ and therefore $\sigma \to -\sigma$. If the statistics of the forcing ξ also obey (15), then (17) is a statistical symmetry of (1) and therefore

$$\sigma(\gamma) = -\sigma(-\gamma). \tag{18}$$

But the symmetry (15) is not compulsory; for example, the single-wave forcing of Ferrari and Nikurashin (2010) and Klocker et al. (2012) does not satisfy (15). However we make the assumption that the forcing is reflexionally symmetric and we proceed confining attention to ξ with statistics obeying (15). As a consequence of this restriction, $\sigma(\gamma)$, calculated explicitly in section 5, satisfies (18).

e. The stochastic forcing

Our main illustrative example is provided by the correlation function

$$\Xi = 2\varepsilon k_f^2 [J_0(k_f r) - \alpha J_2(k_f r) \cos 2\theta], \tag{19}$$

where $(x, y) = r(\cos\theta, \sin\theta)$, k_f is the ''forced wavenumber,'' and $J_m(z)$ is the Bessel function of order m. The corresponding spectrum is

$$\tilde{\Xi}(p, q) = 4\pi k_f \varepsilon (1 + \alpha \cos 2\phi) \delta(k - k_f), \tag{20}$$

with $(p, q) = k(\cos\phi, \sin\phi)$. The forcing is concentrated on a circle with radius k_f in wavenumber space. To ensure that the spectrum is nonnegative, the anisotropy parameter α must satisfy $-1 \le \alpha \le 1$. Figure 1 shows model correlation functions and forcing obtained by varying α in (19).

3. Statistical Galilean invariance

The linearized vorticity equation in (1), with the rapidly decorrelating forcing in (5), has a form of statistical Galilean invariance. To explain this, consider two observers—one of whom is stationary and at the origin of the (x, y, t) coordinate system in (1). The other observer is at $y = b$ and moves ''with the mean flow,'' at speed γb along the axis of x relative to the first. Because of the rapid temporal decorrelation of the forcing ξ, these two observers see statistically identical versions of the problem (1). Thus all zonally averaged quantities are
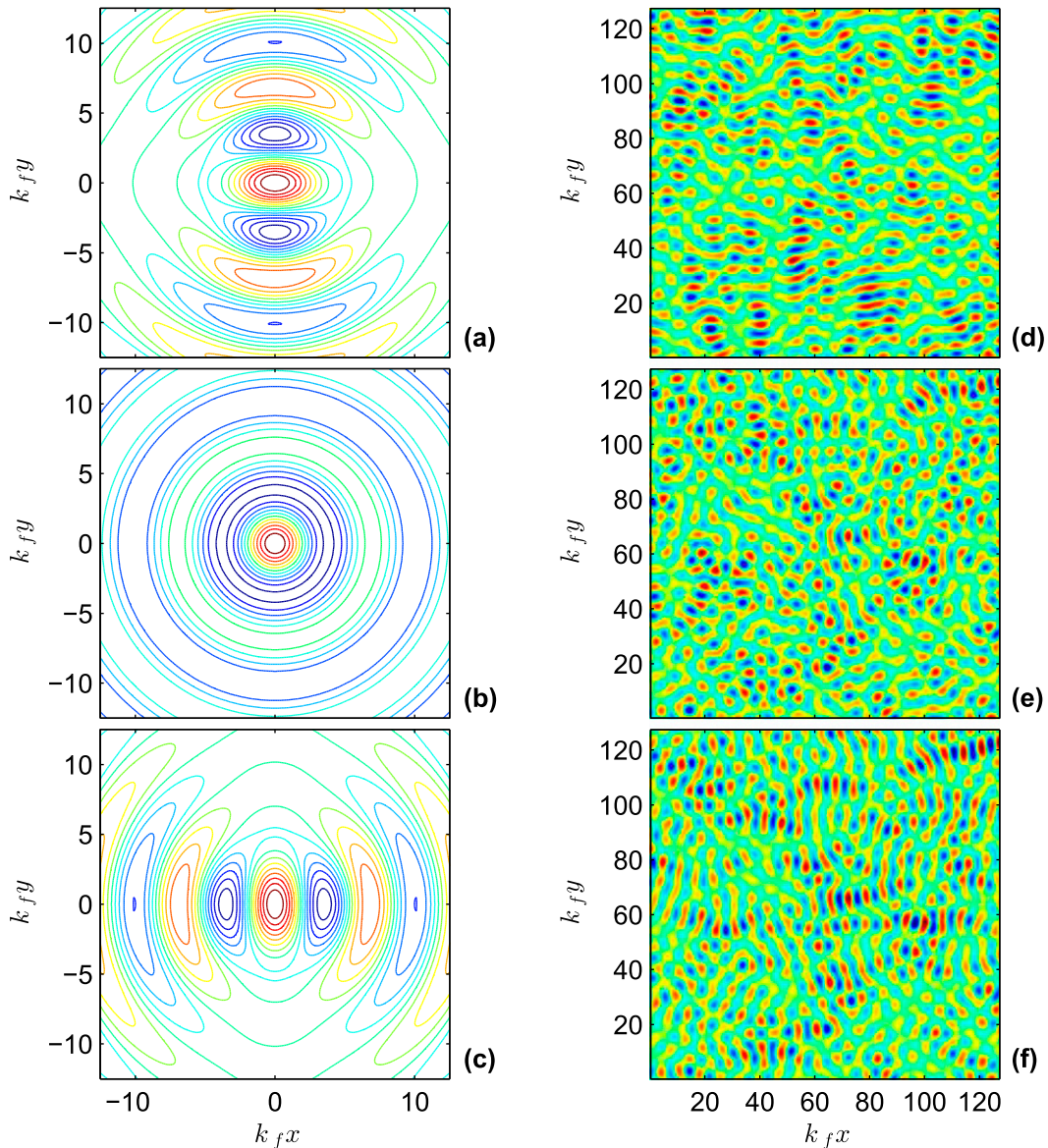
FIG. 1. (a)–(c) Plots of Ξ in (19) and (d)–(f) corresponding snapshots of ξ for (a),(d) $\alpha = -1$, (b),(e) the isotropic case $\alpha = 0$, and (c),(f) $\alpha = +1$.

independent of y. This simple argument allows us to anticipate some curious aspects of the detailed calculations that follow in section 5.

Notice that if the forcing has a nonzero temporal decorrelation time then the statistical properties of ξ are different in the two frames of reference, and consequently the problem is no longer statistically Galilean invariant (or even Galilean invariant). If there is a nonzero decorrelation time, then averaged quantities do depend on y. A clear example is steady forcing, such as $\xi = \cos k_f x$ used by Manfroi and Young (1999). In the frame of the observer at $y = b$, this forcing is periodic in

time. In this example, the forcing breaks Galilean invariance because there is a special frame in which the forcing is steady (or has the longest decorrelation time in the stochastic case).

To formally prove statistical Galilean invariance, suppose that the second observer above uses coordinates $(\tilde{x}, \tilde{y}, \tilde{t})$. The relation between the two coordinate systems is

$$\tilde{x} = x - \gamma b t, \quad \tilde{y} = y - b, \quad \tilde{t} = t. \tag{21}$$

In the "tilde frame" the equation of motion (1) is

$$\zeta'_{\tilde{t}} + \gamma \tilde{y} \zeta'_{\tilde{x}} + \beta v' + \mu \zeta' = \xi(\tilde{x} + \gamma bt, \tilde{y} + b, \tilde{t}). \quad (22)$$

If the right-hand side of (22) has the same statistical properties as $\xi(x, y, t)$ in (1), then this Galilean transformation is a statistical symmetry. And indeed, because of the $\delta(t_1 - t_2)$ correlation in (5), this is the case.

The important consequence of statistical Galilean invariance is that zonally averaged quantities are independent of y, despite the explicit y dependence in (1) and (2). As an application of this result, the eddy vorticity flux is related to the Reynolds stress by the Taylor identity

$$\overline{v' \zeta'} = -(\overline{u' v'})_y. \quad (23)$$

Because $\overline{u' v'}$ is independent of y, it follows that the statistically steady solution of (1) must have

$$\overline{v' \zeta'} = 0. \quad (24)$$

That is, there is no eddy flux of vorticity, even though the planetary vorticity βy is stirred by eddies [but see the discussion surrounding (45)].

4. Power integrals

a. Enstrophy

The enstrophy power integral is obtained by multiplying (1) by ζ' and zonally averaging. Using (24), the result is

$$\mu \overline{\zeta'^2} = \overline{\xi \zeta'}. \quad (25)$$

Because there is no production of eddy enstrophy by stirring of the β gradient, there is a strict balance in (25) between local eddy enstrophy production on the right-hand side and enstrophy dissipation by drag on the left-hand side.

b. Energy

The energy power integral is obtained by multiplying the vorticity equation [see (1)] by ψ' and zonally averaging. Again, because of statistical Galilean symmetry, zonally averaged quantities, such as $\overline{u'^2}$, are independent of y and one finds

$$\gamma \overline{u' v'} = \varepsilon - \mu(\overline{u'^2} + \overline{v'^2}). \quad (26)$$

The left-hand side of (26) is the transfer of energy between the eddies and the shear flow. The first term on the right-hand side of (26),

$$\varepsilon \stackrel{\text{def}}{=} -\overline{\psi' \xi}, \quad (27)$$

is the rate of working of the stochastic force. Because the forcing is white in time, ε in (27) is the same as ε in (19) and (20). A more detailed discussion of this aspect can be found in Srinivasan and Young (2012).

c. Tracer variance

The tracer variance equation is obtained by multiplying the scalar equation [see (2)] by c' and zonally averaging:

$$\beta_c \overline{v' c'} + \mu \overline{c'^2} = 0. \quad (28)$$

Thus, $\kappa_e = \mu \overline{c'^2}/\beta_c^2$: the tracer eddy diffusivity is nonzero and positive. Taylor's analogy between eddy transport of vorticity and eddy transport of scalars fails: according to (24) there is no eddy flux of vorticity, while from (28), there must be a downgradient tracer flux.

d. Covariance of tracer and vorticity

The fourth and final power integral is obtained by "cross multiplying" the vorticity equation [see (1)] and the scalar equation [see (2)]:

$$\beta \overline{v' c'} + 2\mu \overline{c' \zeta'} = 0, \quad (29)$$

and therefore $\kappa_e = 2\mu \overline{\zeta' c'}/\beta \beta_c$. The power integral in (29) relates the tracer eddy flux to the covariance $\overline{c' \zeta'}$ and, in combination with (28), shows that $2\beta_c \overline{c' \zeta'} = \beta \overline{c'^2} > 0$.

e. A bound on the Reynolds stress

Combining the energy power integral in (26) with the inequality $\overline{u'^2} + \overline{v'^2} \geq 2\overline{u' v'}$, we obtain

$$\sigma \leq \frac{\varepsilon}{\gamma + 2\mu}. \quad (30)$$

This bound on the Reynolds stress is important because it is independent of the details of the forcing (i.e., the model for Ξ) and because in (44) below, the bound is saturated.

f. Bounds on the eddy diffusivity

Combining the tracer variance power integral (28) with the Cauchy–Schwarz inequality,

$$|\overline{v' c'}| \leq \sqrt{\overline{c'^2} \; \overline{v'^2}}, \quad (31)$$

we obtain

$$\kappa_e \leq 2\kappa_v, \quad (32)$$

where

$$\kappa_v \overset{\text{def}}{=} \frac{\overline{v'^2}}{2\mu}. \tag{33}$$

Another bound on κ_e is obtained by combining the covariance integral in (29) with the Cauchy–Schwarz inequality for $\overline{\zeta'\,c'}$. One finds

$$\kappa_e \lesssim 2\kappa_\zeta, \tag{34}$$

where

$$\kappa_\zeta \overset{\text{def}}{=} \frac{2\mu\overline{\zeta'^2}}{\beta^2}. \tag{35}$$

A more elaborate analysis in appendix A shows that (33) and (35) can be combined into a single stronger inequality

$$\kappa_e \leq \frac{2\kappa_v\kappa_\zeta}{\kappa_v + \kappa_\zeta}, \tag{36}$$

or equivalently in terms of harmonic averages

$$\frac{1}{\kappa_e} \geq \frac{1}{2}\left(\frac{1}{\kappa_v} + \frac{1}{\kappa_\zeta}\right). \tag{37}$$

We will see later that the bounds above are typically too generous by a factor of 2.

The four power integrals, and the ensuing bounds on σ and κ_e, provide important and general connections between quadratic statistics characterizing the main properties of the flow. However, these relations are unclosed and to make further progress, we consider the dynamics of correlation functions.

5. Reynolds stress and anisotropy

An evolution equation for $\mathcal{Z}$ in (7) is obtained using the replica trick: take (1) at point 1 and multiply by ζ'_2 and vice versa. Adding these two expressions and then zonally averaging one finds

$$\gamma y \partial_x \mathcal{Z} = \Xi - 2\mu\mathcal{Z}. \tag{38}$$

The enstrophy and energy power integrals in (25) and (26) are immediately recovered by evaluating (38), and the inverse Laplacian[1] of (38), at zero separation.

---

[1] Note that (38) can be written identically as $\gamma\nabla^2(y\nabla^2\Psi_x - 2\Psi_{xy}) = \Xi - 2\mu\nabla^4\Psi$. One can take the inverse Laplacian with impunity because there are no zero eigenmodes.
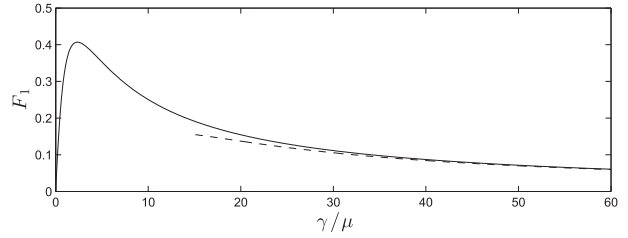

FIG. 2. Plot of F_1 in (42) as a function of γ/μ. The dashed curve is the approximation $F_1(\gamma/\mu) = 4\mu/\gamma - 8\pi\mu^2/\gamma^2 + O[\mu^3/\gamma^3 \ln(\mu/\gamma)]$.

A surprising aspect of (38) is the lack of a term containing β: the β term that would appear in the left-hand side of (38), on performing the replica trick mentioned above, is

$$\beta(\overline{v'_1\zeta'_2} + \overline{v'_2\zeta'_1}) = \beta(\partial_{x_1} + \partial_{x_2})\nabla^2\Psi. \tag{39}$$

The term above is zero because, owing to the homogeneity property of Ψ in section 2a, $\partial_{x_1} = -\partial_{x_2} = \partial_x$. For a more detailed and general derivation of (38), see Srinivasan and Young (2012).

Once one has the solution of (38), the Reynolds stress is given by

$$\overline{u'\,v'} = \Psi_{xy}(0,0). \tag{40}$$

It is remarkable that the vorticity correlation equation in (38) is independent of β; that is, anisotropic Rossby wave propagation does not affect the vorticity correlation function $\mathcal{Z}(x, y)$ nor the Reynolds stress in (40). Thus, all results in this section, which follow from the solution of (38) alone, apply to β-plane flows, even though the parameter β does not appear.

a. Reynolds stress

A general solution of (38) is detailed in appendix B. With the anisotropic ring forcing in (15), the Reynolds stress $\sigma = \overline{u'v'}$ obtained from (40) is

$$\sigma = \frac{\varepsilon\alpha}{4\mu}F_1\left(\frac{\gamma}{\mu}\right), \tag{41}$$

where the function F_1 is

$$F_1\left(\frac{\gamma}{\mu}\right) \overset{\text{def}}{=} 4\mu\gamma \int_0^\infty \frac{\tau^2 e^{-\tau}}{16\mu^2 + \gamma^2\tau^2}\,d\tau. \tag{42}$$

The function F_1 can be expressed in terms of the exponential integral (see appendix C) and is shown in Fig. 2.

We emphasize the linear dependence of σ in (41) on α. In particular, if $\alpha = 0$ (isotropic forcing), there is no

Reynolds stress. This recapitulates the result that anisotropic forcing, or initial conditions, is essential to the generation of nonzero Reynolds stress (Kraichnan 1976; Shepherd 1985; Farrell and Ioannou 1993; Holloway 2010; Cummins and Holloway 2010; Srinivasan and Young 2012).

The Reynolds stress in (41) depends nonlinearly on γ and thus the concept of an eddy viscosity is not generally useful. Instead, there is a nonlinear, and nonmonotonic, stress–strain relation encoded in F_1. However in the weak-shear limit, $\gamma/\mu \ll 1$, the integral in (42) simplifies and the Reynolds stress is then

$$\sigma \approx \underbrace{\frac{\varepsilon\alpha}{8\mu^2}}_{=-\nu_e}\gamma. \tag{43}$$

The sign of the eddy viscosity ν_e is determined by α, with $\alpha > 0$ being the antifrictional case. A negative viscosity in the weak-shear limit, with the same form as (43), was also found by Bakas and Ioannou (2013) using a forcing function that is similar to the $\alpha = 1$ case in this paper.

The integral in (42) also simplifies in the strong-shear limit $\gamma/\mu \gg 1$, reducing to

$$\sigma \approx \frac{\varepsilon\alpha}{\gamma}. \tag{44}$$

The inverse dependence of stress on shear in the strong-shear limit is striking. This might be interpreted as an indication that strong shear is rapidly pushing wavy disturbances into the Farrell and Ioannou's "unfavorable" sector of the wavenumber plane, where they damp away because of the Kelvin–Orr mechanism.[2] But as we show in the next section, a complicating factor is the dependence of the kinetic energy density on the shear.

Another interpretation of (44) is that if $\alpha = \pm 1$, then the Reynolds stress bound in (30) is an asymptotic equality as $\gamma/2\mu \to \infty$. One might say that the γ^{-1} dependence in (44) is the strongest possible Reynolds stress that can be achieved, consistent with the energy power integral (26) and the associated bound (30). Notice that (44) was obtained with the anisotropic ring forcing in (19), but the bound (30), which makes no assumptions about the structure of the forcing, indicates that $\sigma \propto \gamma^{-1}$ is a general result in the strongly sheared limit.

---

[2] In the solution in appendix B, the sheared wavenumber is $q = \hat{q} - p\gamma t$, where $\hat{q}$ is the initial meridional wavenumber. The unfavorable sector is $q < 0$. In this sector, according to the solution of the Kelvin–Orr initial value problem, the energy of the disturbances decreases.

b. The vorticity flux of a slowly varying mean flow

In the discussion surrounding (23) and (24) we argued that $\overline{v'\zeta'}$ is zero. However, if following (6), we view γ as the shear of a slowly varying $U(y)$, then a nonzero $\overline{v'\zeta'}$ can be calculated with our results. Using this "slowly varying" argument, we can write the Reynolds stress as a function of the shear:

$$\overline{u'v'} = \sigma(U_y), \tag{45}$$

where σ is the function in (41). Then using the Taylor identity (23), one has

$$\overline{v'\zeta'} = -\sigma'(U_y)U_{yy}, \tag{46}$$

where σ' is the derivative with respect to γ.

c. Eddy kinetic energy and enstrophy

In addition to the Reynolds stress, the statistically steady solution is characterized by the eddy enstrophy and the eddy kinetic energy. The eddy enstrophy is obtained by evaluating (38) at $\mathbf{x} = 0$ and is simply

$$\overline{\zeta'^2} = \frac{\Xi(0,0)}{2\mu} = \frac{\varepsilon k_f^2}{\mu}. \tag{47}$$

There is no dependence of the eddy enstrophy on the parameter γ/μ (nor on β).

The eddy kinetic energy is obtained from the energy power integral in (26). For anisotropic-ring forcing, the result is

$$\underbrace{\frac{1}{2}(\overline{u'^2} + \overline{v'^2})}_{\overset{\text{def}}{=}E'} = \frac{\varepsilon}{2\mu}\left(1 - \frac{\gamma\alpha}{4\mu}F_1\right). \tag{48}$$

Figure 3a shows the scaled eddy kinetic energy $2\mu E'/\varepsilon$ as a function of γ/μ. The antifrictional case is $\alpha = +1$, with $2\mu E'/\varepsilon < 1$; that is, the eddy kinetic energy is depleted below the unsheared value by transfer to the large-scale shear flow. In the frictional case ($\alpha = -1$), the eddy kinetic energy is enhanced by transfer from the mean flow: the energy level approaches twice that of the isotropically forced flow as the shear increases.

In the strong-shear limit in Fig. 3a, there is much more eddy energy in the frictional flow ($\alpha = -1$) than in the antifrictional flow ($\alpha = +1$). Specifically, if $\gamma/\mu \to \infty$ then, using (C5), the eddy kinetic energy is

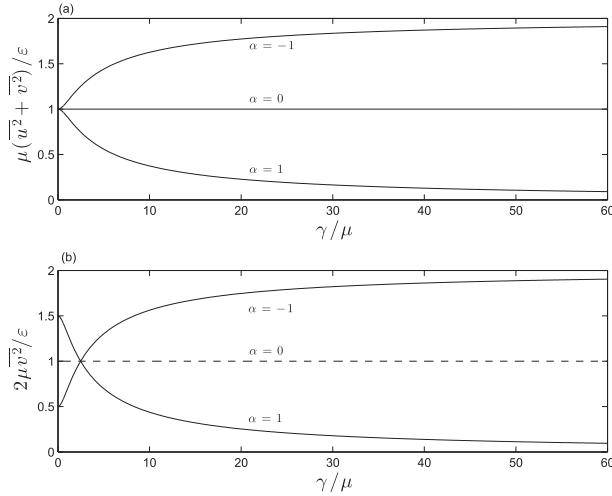$$E' \approx \frac{\varepsilon}{4\mu}\left[(1 - \alpha) + \frac{2\pi\alpha\mu}{\gamma}\right]. \tag{49}$$

FIG. 3. (a) The nondimensional eddy kinetic energy as a function of γ/μ, calculated from (48). (b) The nondimensional meridional velocity variance as a function of γ/μ.
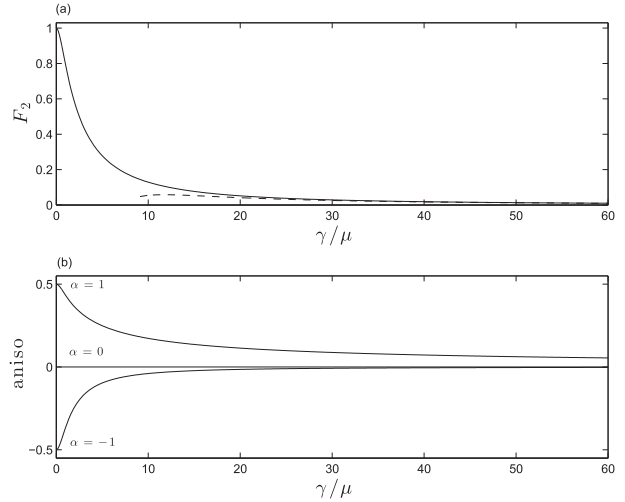

FIG. 4. (a) The function $F_2(\gamma/\mu)$ defined in (51). The dashed curve is the asymptotic approximation $(16\mu^2/\gamma^2)[\ln(\gamma/4\mu) - \gamma_E]$, where $\gamma_E = 0.577\,21\ldots$ is Euler's constant. (b) The index aniso in (52), with $\alpha = -1$, 0, and 1.

This shows that the case $\alpha = 1$ is special: only in this case does the E' vanish in the strong-shear limit. The relatively energetic $\alpha = -1$ eddies are inefficient at forming the requisite correlation to produce a Reynolds stress. This motivates further examination of the anisotropy of the eddies.

d. Velocity anisotropy

In appendix B we show that the mean square meridional velocity is

$$\overline{v'^2} = \frac{\varepsilon}{2\mu}\left[1 + \frac{\alpha}{2}\left(F_2 - \frac{\gamma}{2\mu}F_1\right)\right], \qquad (50)$$

where F_1 is in (42) and

$$F_2\left(\frac{\gamma}{\mu}\right) = 16\mu^2 \int_0^\infty \frac{\tau e^{-\tau}}{16\mu^2 + \gamma^2\tau^2}\,d\tau. \qquad (51)$$

Figure 4a shows F_2 as a function of the nondimensional shear γ/μ, and Fig. 3b shows the variation of the mean-square meridional velocity with γ/μ.

As a nondimensional index of the flow anisotropy, we use the quantity

$$\text{aniso} \stackrel{\text{def}}{=} \frac{\overline{v'^2} - \overline{u'^2}}{\overline{v'^2} + \overline{u'^2}}, \qquad (52)$$

or equivalently

$$\frac{\overline{v'^2}}{\overline{u'^2}} = \frac{1 + \text{aniso}}{1 - \text{aniso}}. \qquad (53)$$

Using (50), the numerator in (52) is

$$\overline{v'^2} - \overline{u'^2} = \frac{\varepsilon\alpha}{2\mu}F_2\left(\frac{\gamma}{\mu}\right). \qquad (54)$$

The dependence of the index aniso in (52) on the shear is shown in Fig. 4b.

In the large-shear limit, the case $\alpha = -1$ in Fig. 4b rapidly tends to isotropy ($\alpha = +1$ also tends to zero, but much more slowly than $\alpha = -1$). This is consistent with the earlier result that the amplitude of the Reynolds stress in (44) is the same for $\alpha = +1$, as for $\alpha = -1$, despite the great difference in the energy level of the two flows as $\gamma/\mu \to \infty$. In other words, with $\alpha = -1$, the eddies are energetic but almost isotropic and are therefore not very efficient at producing a nonzero Reynolds stress.

e. Tenacity of isotropy

Figure 4b shows that if the forcing is isotropic ($\alpha = 0$), then the flow is also isotropic; that is, if the flow is isotropically forced, then neither the mean shear nor the β effect induces anisotropy of the eddies. Moreover, if the forcing is anisotropic, then the effect of shear is to make the flow more isotropic: in both Fig. 4a and 4b, the index of flow anisotropy approaches zero monotonically as γ/μ increases. We cannot provide an intuitive explanation of this result.

For a recent discussion of isotropy in the context of fully nonlinear sheared turbulence, see Cummins and Holloway (2010): a main point is that nonlinear eddy–eddy interactions also decrease anisotropy. We summarize all these results by saying that isotropy is tenacious.

6. Eddy diffusivity

We turn now to the eddy diffusivity, viewed as a function of the four main parameters: $\kappa_e(\alpha, \beta, \gamma, \mu)$. Using the replica trick, one can obtain evolution equations for the tracer correlation functions defined in (9) and (10). Combining (1) and (2) one has

$$\gamma y \nabla^2 P_x + \beta P_x + 2\mu \nabla^2 P = \beta_c \nabla^2 \Psi_x, \qquad (55)$$

and from (2) alone, one has

$$\gamma y C_x + 2\mu C = -\beta_c (P_x - Q_x). \qquad (56)$$

The equation for Q is obtained by $P \to Q$ and $(x, y) \to -(x, y)$ in (55). After solving (55), the tracer diffusivity defined in (4), is obtained as

$$\kappa_e = -\frac{P_x(0,0)}{\beta_c}. \qquad (57)$$

The solution of (55), and the calculation of the tracer diffusivity defined in (4), is summarized in appendix D. The result is

$$\kappa_e = \frac{1}{\beta^2} \iint \tilde{\Xi}(p,q)\tilde{M}(p,q)\frac{dp\,dq}{(2\pi)^2}; \qquad (58)$$

the kernel in (58) is

$$\tilde{M}(p,q;\beta,\gamma,\mu) = 1 - 2\mu \int_0^\infty e^{-2\mu t}\cos\chi\,dt, \qquad (59)$$

with the phase

$$\chi = \frac{\beta}{\gamma p}\left[\arctan\left(\frac{q}{p} - \gamma t\right) - \arctan\left(\frac{q}{p}\right)\right]. \qquad (60)$$

a. The case $\gamma = \beta = 0$

If $\beta = \gamma = 0$, then we do not need the complicated expressions for κ_e above: cancel ∇^2 in (55) and then take an x derivative to obtain

$$\kappa_e(\alpha, 0, 0, \mu) = \underbrace{\frac{\overline{v'^2}}{2\mu}}_{\kappa_v}, \qquad (61)$$

where we have used $\overline{v'^2} = \Psi_{xx}(0,0)$, and we recalled the definition of κ_v in (33). Notice that the upper bound on κ_e in (32) is too generous by a factor of 2 relative to (61). Using results from section 5, the eddy diffusivity in (61) can also be written as

$$\kappa_e(\alpha, 0, 0, \mu) = \frac{\varepsilon}{4\mu^2}\left(1 + \frac{\alpha}{2}\right); \qquad (62)$$

the dependence of κ_e on the anisotropy α reflects that of $\overline{v'^2}$.

b. The suppression factor

One can view (61) as saying that the eddy diffusivity is the product of a typical meridional eddy velocity, equal to the root-mean-square of v', times the mixing length

$$\sqrt{\overline{v'^2}}\bigg/2\mu. \qquad (63)$$

We adopt this interpretation and express κ_e in terms of κ_v and Ferrari and Nikurashin's (2010) suppression factor S as

$$\kappa_e = \kappa_v S. \qquad (64)$$

In (61), $S = 1$. But the effect of nonzero β and γ is usually to make κ_e less than κ_v.

c. The case $\gamma = 0$

Unlike the Reynolds stress in (41) and the anisotropy in (52), the eddy diffusivity depends on the planetary vorticity gradient. This dependence is illustrated by the special case $\gamma = 0$. With no mean shear, the phase in (60) simplifies to $\chi = \omega t$, where

$$\omega = -\frac{\beta p}{p^2 + q^2} \qquad (65)$$

is the Rossby wave frequency. Thus, the kernel in (59) reduces to

$$\tilde{M}(p,q;\beta,0,\mu) = \frac{\omega^2}{(2\mu)^2 + \omega^2}. \qquad (66)$$

For the anisotropic ring forcing in (19), the $\gamma = 0$ tracer diffusivity obtained from the integral in (58) is then

$$\kappa_e(\alpha, \beta, 0, \mu) = \frac{\varepsilon}{4\mu^2}\left(B_0 + \frac{\alpha}{2}\sqrt{1 + \tilde{\beta}^2}B_0^2\right), \qquad (67)$$

where

$$\tilde{\beta} \stackrel{\text{def}}{=} \frac{\beta}{2\mu k_f} \qquad (68)$$

is a nondimensional planetary vorticity gradient and

$$B_0(\tilde{\beta}) \stackrel{\text{def}}{=} \frac{2}{\tilde{\beta}^2}\left(1 - \frac{1}{\sqrt{1 + \tilde{\beta}^2}}\right). \qquad (69)$$
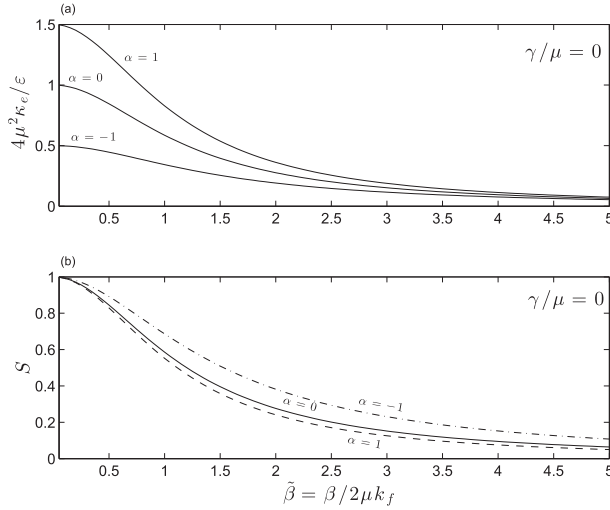
FIG. 5. (a) The nondimensional $\gamma = 0$ tracer diffusivity in (67) as a function of $\tilde{\beta} = \beta/(2\mu k_f)$. (b) The suppression factor, defined in (70).

Following (64), the eddy diffusivity in (67) can alternatively be written as

$$\kappa_e(\alpha, \beta, 0, \mu) = \underbrace{\frac{\overline{v'^2}}{2\mu}}_{\kappa_v} \underbrace{\frac{2B_0 + \alpha\sqrt{1 + \tilde{\beta}^2}B_0^2}{2 + \alpha}}_{S} . \quad (70)$$

Figure 5a shows the eddy diffusivity in (67) as a function of β, and Fig. 5b shows the factor S in (70). Increasing β reduces both measures of the tracer diffusivity.

The dependence of κ_e on α in Fig. 5a is intuitive: in Fig. 1f, $\alpha > 0$ forces meridionally elongated eddies resulting in enhanced diffusive fluxes in the y direction. The difference between $\alpha = 1$ and $\alpha = -1$ is a factor of 3 in diffusivity at $\tilde{\beta} = 0$, but the dependence on α is reduced as $\tilde{\beta}$ increases.

When $\tilde{\beta} \to \infty$:

$$B_0(\tilde{\beta}) = 2\tilde{\beta}^{-2} + O(\tilde{\beta}^{-3}), \quad (71)$$

and therefore for large $\tilde{\beta}$, the eddy diffusivity is

$$\kappa_e(\alpha, \beta \to \infty, 0, \mu) = \frac{\varepsilon}{4\mu^2}\frac{2}{\tilde{\beta}^2}, \quad (72)$$

$$= \underbrace{\frac{2\mu\overline{\zeta'^2}}{\beta^2}}_{\kappa_\zeta}, \quad (73)$$

where we have recalled the definition of κ_ζ in (35). The bound (34) is too generous by a factor of 2 relative to (73).

The $\beta \to \infty$ diffusivity in (73) is a general result that is not specific to the anisotropic ring forcing in (20). To see this, we note that if $\beta \to \infty$ then the kernel $\tilde{M}$ in (66) simplifies to

$$\tilde{M}(p, q; \beta \to \infty, 0, \mu) \to 1. \quad (74)$$

Setting $\tilde{M} = 1$ in (70) and substituting for the enstrophy from (47), we arrive at (73).

d. Comparison with Klocker et al. (2012)

The β^{-2} suppression of transport in (73) is via the mechanism of Ferrari and Nikurashin (2010) and Klocker et al. (2012): nonzero β enables Rossby wave propagation so that eddies drift relative to the mean flow. We have used the anisotropic ring forcing in (20), whereas Klocker et al. force a single wave. To fully explain the connection, we briefly consider the single-wave forcing of Klocker et al. with correlation function

$$\Xi(x, y) = 2\varepsilon k_f^2 \cos(p_f x + q_f y). \quad (75)$$

The spectrum is

$$\tilde{\Xi}(p, q) = 4\varepsilon\pi^2 k_f^2[\delta(p - p_f)\delta(q - q_f) \\ + \delta(p + p_f)\delta(q + q_f)], \quad (76)$$

where $k_f^2 = p_f^2 + q_f^2$. Ferrari and Nikurashin (2010) and Klocker et al. (2012) do not have damping in the scalar equation [see (2)], so to see the connection to their work, we replace $\mu c'$ in (2) by $\mu_c c'$. Ferrari and Nikurashin (2010) and Klocker et al. (2012) take $\mu_c = 0$. With $\gamma \neq 0$, this change complicates the expression for the diffusivity in (58). But, for comparison with Klocker et al. (2012), we restrict attention to $\gamma = 0$. Then there is only a minor modification in the tracer correlation equation [see (55)] and the diffusivity formula in (D11): every 2μ term is just replaced by $\mu + \mu_c$. In particular, the kernel $\tilde{M}$ is modified from (66) to

$$\tilde{M}(p, q; \beta, 0, \mu) = \frac{\omega^2}{(\mu + \mu_c)^2 + \omega^2}. \quad (77)$$

The diffusivity integral in (58) is modified by a factor of $(\mu + \mu_c)/2\mu$ and the diffusivity then evaluates to

$$\kappa_e = \frac{p_f^2}{k_f^2}\frac{\mu + \mu_c}{\mu}\frac{\varepsilon}{(\mu + \mu_c)^2 + c_R^2 p_f^2}, \quad (78)$$

where

$$c_R = -\frac{\beta}{k_f^2} \quad (79)$$

is the intrinsic Rossby wave phase speed in the zonal direction. Alternatively, we can express (78) in terms of the meridional velocity variance obtained from (B10),

$$\overline{v'^2} = \frac{\varepsilon p_f^2}{\mu k_f^2}, \tag{80}$$

in the form

$$\kappa_e = \underbrace{\frac{\overline{v'^2}}{\mu + \mu_c}}_{\kappa_v} \underbrace{\frac{1}{1 + c_R^2 p_f^2/(\mu + \mu_c)^2}}_{S} . \tag{81}$$

If $\mu = \mu_c$, then the expression above has the same form as the anisotropic ring diffusivity in (70); if $\mu_c = 0$, then the expression in (78) is identical to (20) in Klocker et al. (2012). Further, in the limit of $\beta \rightarrow \infty$, the general result $\kappa_e \propto \beta^{-2}$ in (73) is recovered by using $\overline{\zeta'^2} = \varepsilon k_f^2/\mu$.

There are two important remarks to make about (81). First, and intuitively, it is $\overline{v'^2}$, rather than the eddy kinetic energy, that determines the unsuppressed eddy diffusivity. Second, it is the intrinsic Rossby wave speed, proportional to the base-state potential vorticity gradient, which appears in the suppression factor. In the model of Klocker et al. (2012), the intrinsic zonal phase speed is

$$c_R = -\frac{\beta + UL_d^{-2}}{k_f^2 + L_d^{-2}}, \tag{82}$$

where U is the background mean flow in the upper layer of their equivalent barotropic model (the lower layer is quiescent) and L_d is the deformation length. Because the potential vorticity gradient, $\beta + UL_d^{-2}$, is modified by the background mean flow, strong mean flow increases c_R and therefore suppresses κ_e. By comparison, in (79), our c_R does not depend on a background mean flow. In both models, it is the meridional potential vorticity gradient, β in (79) and $\beta + UL_d^{-2}$ in (82), that enables eddies to move relative to the mean flow, resulting in a nonzero $c_R = c - U$ and the associated suppression of κ_e. (Note that the Doppler-shifted phase speed c is the observed zonal speed of eddies, as seen, for example, in satellite altimetry.)

e. The case $\beta = 0$

With $\beta = 0$, we evaluate the integrals for κ_e in (58) and (59) numerically. Figure 6a shows $\kappa_e(\alpha, 0, \gamma, \mu)$ as a function of γ/μ. In Fig. 6b, we express the diffusivity in terms of S in (64). The three curves are much closer
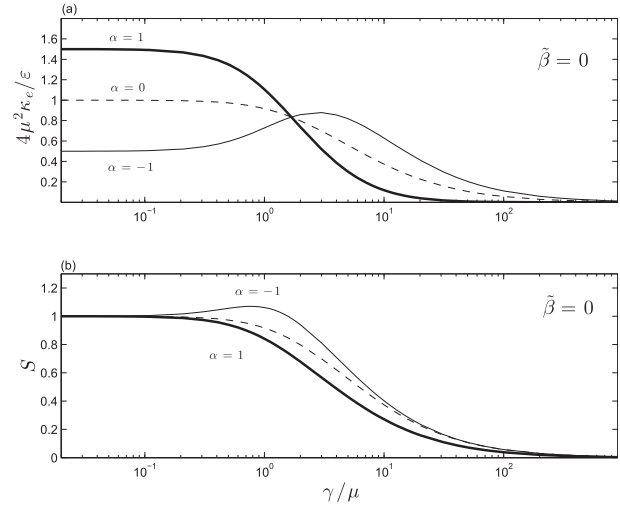

FIG. 6. (a) The nondimensional tracer diffusivity as a function of γ/μ with $\beta = 0$ and different values of α. (b) The corresponding suppression factor defined in (64).

together in Fig. 6b than in Fig. 6a and therefore the variation in κ_e with α and γ/μ is due mainly to variation in $\overline{v'^2}$.

The case $\alpha = -1$ in Fig. 6b shows a slight enhancement of κ_e above κ_v. Thus, in some cases at least, shear can enhance eddy diffusivity, so that S is slightly greater than 1. This weak effect is due to the Kelvin–Orr mechanism: $\alpha = -1$ loads the forcing variance deep in Farrell and Ioannou (1993)'s favorable sector of the wavenumber plane. The diffusivity in (58)–(60) is given by a weighted time integral of the v'^2 associated with a sheared wave. Apparently, this time integral is not necessarily bounded above κ_v (though it is by $2\kappa_v$).

f. Large shear

When $\tilde{\gamma} \gg 1$, and provided $\tilde{\gamma} \gg \tilde{\beta}$, the kernel $\tilde{M}$ in (59) is concentrated near $\phi = \pi/2$, and the integrals can be evaluated approximately (see appendix E). In this large-shear limit, the eddy diffusivity is

$$\kappa_e(\alpha, \beta, \gamma \rightarrow \infty, \mu) \approx (1 - \alpha)\frac{\pi\varepsilon}{2\gamma\mu} B_1(\pi\tilde{\beta}), \tag{83}$$

where the function B_1 is

$$B_1(b) \stackrel{\text{def}}{=} b^{-2}\left[\pi b - 2b\arctan\frac{1}{b} - \ln(1 + b^2)\right]. \tag{84}$$

Figure 7a shows the variation of $B_1(\pi\tilde{\beta})$ with $\tilde{\beta}$ while Fig. 7b shows that the approximate expression in (83) is in good agreement with numerical computation of κ_e using (58).
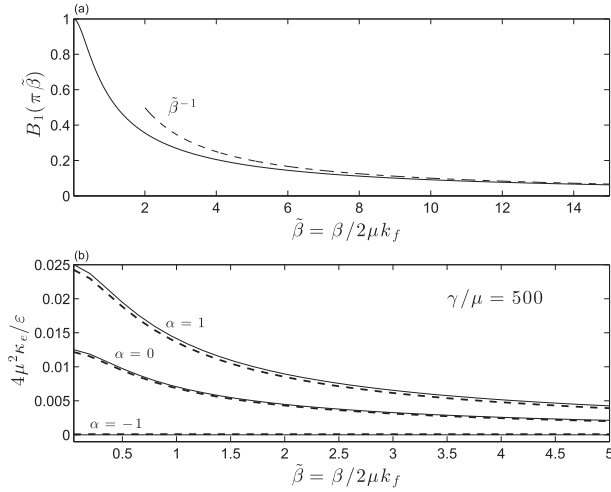
FIG. 7. (a) The function $B_1(\pi\tilde{\beta})$ given in (84) shown as a function of $\tilde{\beta}$. The large $\tilde{\beta}$ approximation is the dashed curve. (b) A comparison of the numerically computed nondimensional tracer diffusivity for $\gamma/\mu = 500$ (dashed curve) with the approximate expression in (83) (solid curve).

In the limit of large shear, the meridional velocity variance in (50) becomes

$$\overline{v'^2} = \frac{\varepsilon}{2\mu}(1-\alpha) + O(\tilde{\gamma}^{-1}), \qquad (85)$$

and can be used to rewrite the eddy diffusivity in terms of S in the form

$$\kappa_e(\alpha,\beta,\gamma \to \infty, \mu) \approx \kappa_v \underbrace{\frac{2\pi}{\tilde{\gamma}}B_1(\pi\tilde{\beta})}_{S} . \qquad (86)$$

This result leads to two important conclusions: first, $S \propto \gamma^{-1}$; that is, large shear suppresses eddy diffusivity and in the large-shear limit, the γ^{-1} dependence is the same as the earlier result for the Reynolds stress in (44). Second, the effect of anisotropy on the diffusivity is completely included in $\overline{v'^2}$, so that S is independent of α. Limiting forms of the suppression factor in (86) for large and small $\tilde{\beta}$ can be inferred from Fig. 7a as

$$S \approx \begin{cases} \dfrac{2\pi}{\tilde{\gamma}} & \text{if} \quad \tilde{\beta} \to 0, \\[2mm] \dfrac{2\pi}{\tilde{\gamma}\tilde{\beta}} & \text{if} \quad \tilde{\gamma} \gg \tilde{\beta} \gg 1. \end{cases} \qquad (87)$$

Figure 8a shows comparisons of the numerically computed diffusivity integral in (58) for isotropic forcing ($\alpha = 0$), with the asymptotic forms displayed in (87).

Finally, we note that in the limit $\tilde{\beta} \gg \tilde{\gamma} \gg 1$, the general result of (73) is recovered; that is,
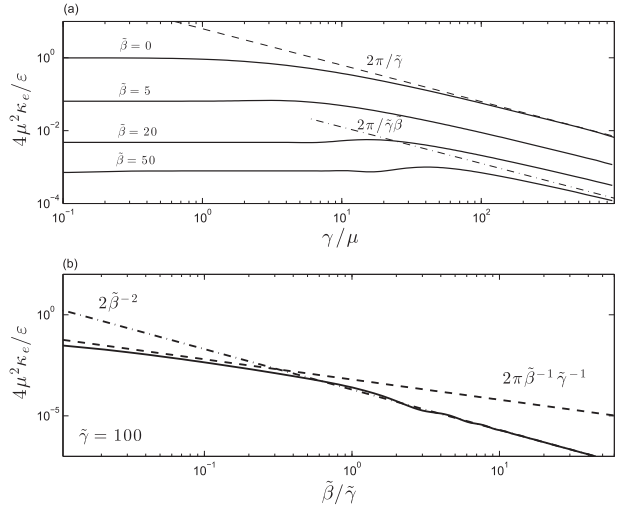

FIG. 8. (a) The numerically computed nondimensional tracer diffusivity as a function of γ/μ, with different values of β, and $\alpha = 0$. Also plotted are the large γ asymptotes for $\tilde{\beta} = 0$ (dashed line) and $\tilde{\beta} = 50$ (dot–dashed line) in (87). (b) Comparison of the numerically computed nondimensional κ_e for $\tilde{\gamma} = 100$ (solid line) as a function of $\tilde{\beta}/\tilde{\gamma}$, with asymptotes corresponding to the limits $\tilde{\beta} \gg \tilde{\gamma} \gg 1$ (dot–dashed line) and $\tilde{\gamma} \gg \tilde{\beta} \gg 1$ (dashed line).

$$\kappa_e = \kappa_\zeta \quad \text{if} \quad \tilde{\beta} \gg \tilde{\gamma} \gg 1. \qquad (88)$$

In Fig. 8b, the normalized eddy diffusivity is plotted as a function of $\tilde{\beta}/\tilde{\gamma}$ for a large value of the shear ($\tilde{\gamma} = 100$). It is clear that when $\tilde{\beta}/\tilde{\gamma}$ is small, the diffusivity asymptotically approaches the lower result in (87) and to (88) [written in the equivalent form, (72)] for large values of $\tilde{\beta}/\tilde{\gamma}$.

7. Discussion and conclusions

The model (1) and (2) has a special status as an analytically tractable example whose solution sheds light on eddy transport of momentum, vorticity, and tracer. To be sure, the model is linear and, unless one has strong faith in stochastic turbulence models, the results might therefore apply only in the case of weak, externally forced eddies in a strong mean flow. We caution also that the Kelvin–Orr mechanism is quite special to the infinite shear flow $U = \gamma y$: at first, a wave "leaning into the shear" gains energy from the mean. Ultimately, the energy is returned as the shear tilts the wave into the unfavorable quadrant; that is, U has no discrete shear modes that serve as a repository for eddy energy. The next step is to consider the eddy diffusivity and Reynolds stresses of more structured shear flows.

Key results for (1) and (2) detailed in this paper emphasize the dependence of the statistical properties of the solutions of the linear vorticity equation [see (1)]

and the scalar equation [see (2)] on the spatial structure of the forcing ξ and the shear γ. However, the role of β is peculiar: a great and unexpected simplification is that the eddy kinetic energy level and the Reynolds stress σ are independent of β. But σ is a nonlinear and nonmonotonic function of the γ. Thus, while it is sensible to define an eddy diffusivity according to (4), one cannot define an analogous eddy viscosity because σ is not linearly proportional to γ. Thus, our result for σ in (41) provides an explicit analytic example of Dritschel and McIntyre (2008)'s "antifriction" (as opposed to negative eddy viscosity).

The spatial structure of ξ is characterized by the anisotropy parameter α in (19). The Reynolds stress is found to be directly proportional to α, so "frictional" and "antifrictional" stresses are obtained when α is negative and positive, respectively. And if the forcing is isotropic, then the Reynolds stress is identically zero. When γ is weak, the Reynolds stress is proportional to γ. Thus, in this special case, one can identify an effective viscosity ν_e whose sign is opposite to that of α. The expression for ν_e in (43) connects with a similar result obtained by Bakas and Ioannou (2013) for a forcing function resembling our $\alpha = 1$: in this case $\nu_e < 0$.

In general, the most important determinants of the tracer eddy diffusivity κ_e are the meridional kinetic energy $\overline{v'^2}$ and the drag μ. With $\beta = \gamma = 0$, the diffusivity is precisely $\overline{v'^2}/(2\mu)$. But typically, κ_e is smaller than $\overline{v'^2}/(2\mu)$ whenever β or γ are nonzero. In other words, both γ and β suppress eddy diffusivity. If $\gamma = 0$, then the suppression due to β is a consequence of propagation of Rossby waves relative to a background mean flow. The suppression of diffusivity due to β (or more generally, any background potential vorticity gradient) has been discussed previously by Klocker et al. (2012), and their results can be interpreted as a special case of ours with $\gamma = 0$. Strong shear also causes the diffusivity to decrease as γ^{-1}, and this inverse proportionality mirrors the γ^{-1} variation of the Reynolds stress for large γ.

We caution against summarizing the results above by saying that "mean flow suppresses eddy diffusivity." The mean flow is γy and "mean-flow suppression" invites the incorrect conclusion that κ_e would decrease as $|y|$ increases. Instead, fundamentally because of the Galilean invariance in section 3, κ_e is independent of y. The mean-flow suppression explained in Klocker et al. (2012) and Ferrari and Nikurashin (2010) is caused by the relative motion of eddies with respect to the mean flow. However, this relative motion is due to a nonzero potential vorticity gradient, which in the case of Klocker et al. (2012) includes both β and a term resulting from the baroclinic shear of the mean flow. If a barotropic mean flow $U(y)$ has $U_{yy} \neq 0$, then the background

potential vorticity gradient is modified to $\beta - U_{yy}$, and it is this total gradient (rather than just β) that is relevant for eddy suppression. Thus, it is not the mean flow directly, but rather the contribution of the mean flow to the PV gradient that results in suppression of diffusivity.

We close by remarking that our results bear on the historical controversy between Prandtl's theory of momentum transfer and Taylor's theory based on vorticity transfer. The debate migrated into geophysical fluid dynamics in the 1970s (Welander 1973; Thomson and Stewart 1977; Stewart and Thomson 1977) and has recently been recalled by Maddison and Marshall (2013). The results here do not support Taylor's view. Taylor argued that in ideal two-dimensional fluid dynamics, vorticity should be transferred much like a passive scalar and thus advocated an eddy closure that, in our notation, is

$$\overline{v'\zeta'} = -\kappa_e \beta. \tag{89}$$

A prominent problem with this proposal has always been that because of the identity (23), momentum is not conserved on a β plane. Our results pile on more: although the passive scalar eddy diffusivity is nonzero, the vorticity flux on the left-hand side of (89) is zero. Moreover, in general agreement with Prandtl's views, there is a nonzero momentum flux that is, painfully for Taylor, independent of the mean potential vorticity gradient β. Thus, in the model solved here, β is an important control on passive scalar transport, but it is irrelevant for momentum transport.

APPENDIX A

A Bound on Eddy Diffusivity

In addition to the definition in (4), the eddy diffusivity can be obtained from the power integrals in (28) and (29). Thus, we can write the eddy diffusivity as a linear combination of three different expressions:

$$\kappa_e = p\frac{\mu\overline{c'^2}}{\beta\beta_c} + 2q\frac{\mu\overline{\zeta'c'}}{\beta\beta_c} - r\frac{\overline{v'c'}}{\beta_c}, \tag{A1}$$

where $p + q + r = 1$. Completing the square involving c', assuming that $p < 0$, and then dropping the squared term (which has the same sign as p) gives the inequality

$$\kappa_e \le \frac{1}{2} \frac{q^2 \kappa_\zeta + r^2 \kappa_v}{q + r - 1}, \qquad (A2)$$

where κ_v and κ_ζ are defined in (33) and (35). Minimizing the right-hand side of (A2) over q and r, we find

$$q = \frac{2\kappa_v}{\kappa_v + \kappa_\zeta}, \quad r = \frac{2\kappa_\zeta}{\kappa_v + \kappa_\zeta}, \qquad (A3)$$

and therefore $p = -1$. The smallest value of the right-hand side of (A2) produces the best upper bound on κ_e, which is the result in (36).

APPENDIX B

Details of the $\mathcal{Z}$ Solution

Using the convention in (12), the Fourier transform of (38) is

$$-\gamma p \tilde{\mathcal{Z}}_q = \tilde{\Xi} - 2\mu \tilde{\mathcal{Z}}. \qquad (B1)$$

The solution of the ordinary differential equation in (B1) can be written as the time integral of a "sheared disturbance":

$$\tilde{\mathcal{Z}}(p, q) = \int_0^\infty e^{-2\mu t} \tilde{\Xi}(p, \hat{q}) \, dt, \qquad (B2)$$

where

$$\hat{q} \stackrel{\text{def}}{=} q + p\gamma t. \qquad (B3)$$

a. A polar representation of $\tilde{\Xi}$

It is convenient to use a polar representation of the spectrum

$$\tilde{\Xi} = \tilde{\Xi}_0(k) + \sum_{n=1}^\infty \tilde{\Xi}_{2n}(k) \cos 2n\phi \qquad (B4)$$

above $p = k \cos\phi$ and $q = k \sin\phi$. The anisotropic ring forcing in (12) has this form. Because of the exchange symmetry [see (11)], only even terms appear within the sum on the right-hand side of (B4). And because of the assumed reflexion symmetry in (15) there are no $\sin 2n\phi$ terms in (B4).

b. The Reynolds stress

In wavenumber space, the Reynolds stress in (40) is

$$\overline{u' v'} = -\iint \frac{pq \tilde{\mathcal{Z}}(p, q)}{(p^2 + q^2)^2} \frac{dp \, dq}{(2\pi)^2}. \qquad (B5)$$

Combining (B2) and (B5) we obtain

$$\gamma \overline{u' v'} = \varepsilon - \mu \iint J_1(p, q) \tilde{\Xi}(p, q) \frac{dp \, dq}{(2\pi)^2}, \qquad (B6)$$

where the kernel is

$$J_1(p, q) \stackrel{\text{def}}{=} \int_0^\infty \frac{e^{-2\mu t}}{p^2 + (q - p\gamma t)^2} \, dt. \qquad (B7)$$

The three terms in (B6) correspond to the three terms in the energy power integral (26).

Substituting the Fourier series expansion of $\tilde{\Xi}(p, q)$ in (B4) into (B6), and performing the ϕ integrals using (B16) below, one finds

$$\overline{u' v'} = \frac{\mu}{\gamma^2} \sum_{n=1}^\infty (-1)^{n+1} \mathcal{T}_{2n} \int_0^\infty \frac{\tilde{\Xi}_{2n}(k)}{2\pi k} \, dk. \qquad (B8)$$

The coefficients in (B8) are

$$\mathcal{T}_{2n} = \int_0^\infty e^{-m\tau/2} \left(\frac{\tau}{\sqrt{\tau^2 + 4}}\right)^n T_n \left(\frac{\tau}{\sqrt{\tau^2 + 4}}\right) d\tau, \qquad (B9)$$

where $m \stackrel{\text{def}}{=} 4\mu/\gamma$ and T_n is the Chebyshev polynomial of order n.

When the forcing $\tilde{\Xi}$ is specialized to the anisotropic ring spectrum in (20), only the $n = 1$ term in (B8) is nonzero, and the k integral is trivial. The expression for $\overline{u' v'}$ in (41) is obtained from (B9) with $n = 1$.

Notice that the isotropic part of the spectrum [i.e., $\tilde{\Xi}_0(k)$ in (B4)] does not contribute to the Reynolds stresses in (B8). This recapitulates the result that isotropic forcing of a Couette flow does not produce Reynolds stresses (Farrell and Ioannou 1993; Srinivasan and Young 2012).

c. Anisotropy

We first compute $\overline{v'^2}$ starting from

$$\overline{v'^2} = \iint \frac{p^2 \tilde{\mathcal{Z}}(p, q)}{(p^2 + q^2)^2} \frac{dp \, dq}{(2\pi)^2}. \qquad (B10)$$

Combining (B2) and (B10), we have

$$\overline{v'^2} = \iint J_2(p, q) \tilde{\Xi}(p, q) \frac{dp \, dq}{(2\pi)^2}, \qquad (B11)$$

where the kernel is

$$J_2(p, q) \stackrel{\text{def}}{=} \int_0^\infty \frac{p^2 e^{-2\mu t}}{[p^2 + (q - p\gamma t)^2]^2} \, dt. \qquad (B12)$$

Owing to the complexity of the kernel $J_2(p, q)$, we compute $\overline{v'^2}$ only for the special case of the anisotropic ring spectrum in (20). On combining with (B11) and evaluating the angular integral as a special case of (B17) gives

$$\overline{v'^2} = \frac{\varepsilon}{2\mu}\left[1 + 2\alpha\int_0^\infty e^{-\tau}B\left(\frac{\gamma\tau}{2\mu}\right)d\tau\right], \quad \text{(B13)}$$

where the function B is defined in (B20). Using $\overline{v'^2} - \overline{u'^2} = 2\overline{v'^2} - (\overline{u'^2} + \overline{v'^2})$, and the expression for the eddy kinetic energy in (48), we obtain $\overline{v'^2} - \overline{u'^2}$ in (54).

d. Two angular integrals

Although the Fourier integral

$$A_n(t) \overset{\text{def}}{=} \oint \frac{e^{2in\phi}}{\cos^2\phi + (\sin\phi - t\cos\phi)^2}\frac{d\phi}{2\pi} \quad \text{(B14)}$$

defeats Mathematica, $A_n(t)$ can be evaluated using the method of residues:

$$A_n(t) = \left[-\frac{t(t-2i)}{t^2+4}\right]^n, \quad (n = 0, 1, 2, \dots). \quad \text{(B15)}$$

If $n \geq 1$, real and imaginary parts of (B15) are separated as

$$A_n(t) = (-1)^n\left(\frac{t}{\sqrt{t^2+4}}\right)^n\left[T_n\left(\frac{t}{\sqrt{t^2+4}}\right)\right.$$
$$\left. - \frac{2i}{\sqrt{t^2+4}}U_{n-1}\left(\frac{t}{\sqrt{t^2+4}}\right)\right], \quad \text{(B16)}$$

where U_{n-1} is the modified Chebyshev polynomial.

An integral required for the evaluation of $\overline{v'^2}$ is

$$B_n(t) \overset{\text{def}}{=} \oint \frac{\cos^2\phi\, e^{2in\phi}}{[\cos^2\phi + (\sin\phi - t\cos\phi)^2]^2}\frac{d\phi}{2\pi}. \quad \text{(B17)}$$

The method of residues gives

$$B_0(t) = \frac{1}{2} \quad \text{(B18)}$$

and

$$B_n(t) = -\left[-\frac{t(t-2i)}{t^2+4}\right]^n\left[\frac{1}{2} + \frac{n}{t(t+2i)}\right], \quad \text{(B19)}$$

where $n = 1, 2, \dots$. Although (B19) can be separated into real and imaginary parts along the lines of (B16), the resulting expression is long and is not stated here. Instead, for the special case of $n = 1$, we have

$$B(t) \overset{\text{def}}{=} \Re B_1(t) = \frac{8}{(t^2+4)^2} - \frac{t^2}{4(t^2+4)} - \frac{1}{4}. \quad \text{(B20)}$$

APPENDIX C

Properties of F_1 and F_2

The functions F_1 in (42) and F_2 in (51) can be written compactly in terms of the exponential integral

$$E(z) \overset{\text{def}}{=} \int_z^\infty \frac{e^{-u}}{u}du, \quad \text{(C1)}$$

and the parameter $m \overset{\text{def}}{=} 4\mu/\gamma$, as

$$F_1(\gamma/\mu) = m + m^2\Im e^{im}E(im), \quad \text{(C2)}$$

$$F_2(\gamma/\mu) = m^2\Re e^{im}E(im). \quad \text{(C3)}$$

(Although the formula above is compact in terms of m, in the main text we use the more natural nondimensional group γ/μ.) We record some useful approximations. If $\gamma/\mu \to \infty$ then

$$F_2\left(\frac{\gamma}{\mu}\right) \sim \frac{16\mu^2}{\gamma^2}\left[\ln\left(\frac{\gamma}{4\mu}\right) - \gamma_E\right] + O\left(\frac{\mu^3}{\gamma^3}\right), \quad \text{(C4)}$$

$$F_1\left(\frac{\gamma}{\mu}\right) \sim \frac{4\mu}{\gamma} - \frac{8\pi\mu^2}{\gamma^2} + O\left[\frac{\mu^3}{\gamma^3}\ln\left(\frac{\gamma}{\mu}\right)\right]. \quad \text{(C5)}$$

APPENDIX D

Details of the Solution for κ_e

It is convenient to use the tracer–vorticity correlation function

$$H \overset{\text{def}}{=} \overline{\zeta_1 c_2} = \nabla^2 P. \quad \text{(D1)}$$

In terms of H, the Fourier transform of (55) is

$$-\gamma p\tilde{H}_q + (i\omega + 2\mu)\tilde{H} = i\frac{\beta_c}{\beta}\omega\tilde{\mathcal{Z}}, \quad \text{(D2)}$$

where

$$\omega(p, q) \overset{\text{def}}{=} -\frac{\beta p}{p^2 + q^2} \quad \text{(D3)}$$

is the Rossby wave frequency. Using the method of characteristics, the solution of (D2) is

$$\tilde{H}(p,q) = i\frac{\beta_c}{\beta} \int_0^\infty \tilde{Z}(p,\hat{q})\omega(p,\hat{q})e^{-2\mu t - i\eta(p,q,t)} \, dt, \quad \text{(D4)}$$

where $\hat{q} \stackrel{\text{def}}{=} q + p\gamma t$ and

$$\eta(p,q,t) \stackrel{\text{def}}{=} \int_0^t \omega(p, q + p\gamma t') \, dt'. \quad \text{(D5)}$$

Noting that $\omega(p,\hat{q}) = \partial_t \eta$, one can integrate by parts in (D4) and obtain a simpler expression for $\tilde{H}$:

$$\tilde{H}(p,q) = \frac{\beta_c}{\beta} \left[\tilde{Z}(p,q) - \int_0^\infty e^{-2\mu t - i\eta} \tilde{\Xi}(p,\hat{q}) \, dt \right]. \quad \text{(D6)}$$

To calculate the eddy diffusivity in (D11) below one needs the integral of $\tilde{H}$ in (D6) over the wavenumbers p and q. The ensuing triple integral is disentangled by changing variables in the wavenumber integrals from (p,q) to $\hat{p} = p$ and $\hat{q} = q + p\gamma t$. One finds

$$\iint \tilde{H}(p,q)\frac{dp \, dq}{(2\pi)^2} = \frac{\beta_c}{\beta} \left[\overline{\zeta'^2} - \iint \tilde{K}(p,q)\tilde{\Xi}(p,q)\frac{dp \, dq}{(2\pi)^2} \right], \quad \text{(D7)}$$

where $\tilde{K}(p,q) = \tilde{K}_r(p,q) + i\tilde{K}_i(p,q)$ is the kernel

$$\tilde{K}(p,q) \stackrel{\text{def}}{=} \int_0^\infty e^{-2\mu t - i\chi(p,q,t)} \, dt, \quad \text{(D8)}$$

with

$$\chi(p,q,t) \stackrel{\text{def}}{=} \int_0^t \omega(p, q - p\gamma t') \, dt'. \quad \text{(D9)}$$

The phase χ is evaluated explicitly in (60). The kernel in (D8) has the symmetry

$$\tilde{K}(p,q) = \tilde{K}^*(-p,-q), \quad \text{(D10)}$$

which shows that $\tilde{K}$ is the Fourier transform of a real function.

Our main goal is to calculate the tracer eddy diffusivity κ_e in (4). Using the power integral (29), this is

$$\kappa_e = \frac{2\mu}{\beta\beta_c} \iint \tilde{H}_r(p,q)\frac{dp \, dq}{(2\pi)^2}, \quad \text{(D11)}$$

where $\tilde{H}_r$ is the real part of $\tilde{H}$. Taking the real part of (D7) we obtain from (D11)

$$\kappa_e = \frac{2\mu\overline{\zeta'^2}}{\beta^2} - \frac{2\mu}{\beta^2} \iint \tilde{K}_r(p,q)\tilde{\Xi}(p,q)\frac{dp \, dq}{(2\pi)^2}. \quad \text{(D12)}$$

Using

$$\overline{\zeta'^2} = \iint \frac{\tilde{\Xi}(p,q)}{2\mu}\frac{dp \, dq}{(2\pi)^2}, \quad \text{(D13)}$$

the result in (D12) is rewritten in (58).

APPENDIX E

Tracer Diffusivity in the Limit $\gamma/\mu \to \infty$

Using the exchange symmetry, we can perform the p and q integrals in (58) over the right half plane $p > 0$, and then multiply by 2. In polar coordinates, we therefore limit attention to $-\pi/2 < \phi < \pi/2$, so that the $\arctan(q/p) = \phi$. As $\gamma/\mu \to \infty$ and $\tilde{\gamma} \gg \tilde{\beta}$, the kernel $\tilde{M}$ in (59) becomes increasingly concentrated close to $\phi = \pi/2$. Indeed, in the distinguished limit $\gamma/\mu \to \infty$, with

$$t_* \stackrel{\text{def}}{=} \frac{1}{\gamma\left(\dfrac{\pi}{2} - \phi\right)} \quad \text{(E1)}$$

fixed and order unity, the phase function in (60) simplifies to

$$\chi \approx -\frac{\beta t_*}{k}\left[\frac{\pi}{2} + \arctan\gamma(t - t_*)\right]. \quad \text{(E2)}$$

Moreover, as γ becomes large, the arctangent above approaches a discontinuous step function with a jump at $t = t_*$. In this limit, the function $\cos\chi(t)$ in (59) is constant on either side of the jump at t_*. This observation enables one to easily perform the integral in (60) with the result

$$\tilde{M}(k,\phi) \approx e^{-2\mu t_*}\left[1 - \cos\left(\frac{\pi\beta t_*}{k}\right)\right]. \quad \text{(E3)}$$

The errors are probably $O(\gamma^{-1})$.

Using the anisotropic ring forcing in (19), we have therefore

$$\kappa_e \approx \frac{2k_f^2\varepsilon}{\pi\beta^2} \int_{-\pi/2}^{\pi/2} \tilde{M}(k_f,\phi)(1 + \alpha\cos2\phi) \, d\phi. \quad \text{(E4)}$$

The main contribution comes from the neighborhood of $\phi = \pi/2$, and after some approximations and transformations,

$$\kappa_e \approx (1-\alpha)\frac{2k_f^2\varepsilon}{\pi\beta^2} \int_0^\infty e^{-2\mu v/\gamma}\left[1 - \cos\left(\frac{\pi\beta v}{k_f\gamma}\right)\right]\frac{dv}{v^2}. \quad \text{(E5)}$$

The integral above can be evaluated exactly:

$$\int_0^\infty e^{-nx}(1-\cos mx)\frac{dx}{x^2}$$
$$=\frac{m}{2}\left[\pi - 2\arctan\frac{n}{m} - \frac{n}{m}\ln\left(1+\frac{m^2}{n^2}\right)\right]. \quad (E6)$$

The result for κ_e is (70).

REFERENCES

Arbic, B. K., and G. R. Flierl, 2004: Effects of mean flow direction on energy, isotropy, and coherence of baroclinically unstable beta-plane geostrophic turbulence. *J. Phys. Oceanogr.,* **34,** 77–93, doi:10.1175/1520-0485(2004)034<0077:EOMFDO>2.0.CO;2.

Bakas, N. A., and P. J. Ioannou, 2013: On the mechanism underlying the spontaneous generation of barotropic zonal jets. *J. Atmos. Sci.,* **70,** 2251–2271, doi:10.1175/JAS-D-12-0102.1.

Boyd, J. P., 1983: The continuous spectrum of linear Couette flow with the beta effect. *J. Atmos. Sci.,* **40,** 2304–2308, doi:10.1175/1520-0469(1983)040<2304:TCSOLC>2.0.CO;2.

Cummins, P. F., and G. Holloway, 2010: Reynolds stress and eddy viscosity in direct numerical simulation of sheared-two-dimensional turbulence. *J. Fluid Mech.,* **657,** 394–412, doi:10.1017/S0022112010001424.

DelSole, T., 2001: A theory for the forcing and dissipation in stochastic turbulence models. *J. Atmos. Sci.,* **58,** 3762–3775, doi:10.1175/1520-0469(2001)058<3762:ATFTFA>2.0.CO;2.

Dritschel, D. G., and M. E. McIntyre, 2008: Multiple jets as PV staircases: The Phillips effect and the resilience of eddy-transport barriers. *J. Atmos. Sci.,* **65,** 855–874, doi:10.1175/2007JAS2227.1.

Farrell, B. F., 1982: The initial growth of disturbances in a baroclinic flow. *J. Atmos. Sci.,* **39,** 1663–1686, doi:10.1175/1520-0469(1982)039<1663:TIGODI>2.0.CO;2.

——, and P. J. Ioannou, 1993: Stochastic forcing of perturbation variance in unbounded shear and deformation flows. *J. Atmos. Sci.,* **50,** 200–211, doi:10.1175/1520-0469(1993)050<0200:SFOPVI>2.0.CO;2.

——, and ——, 2003: Structural stability of turbulent jets. *J. Atmos. Sci.,* **60,** 2101–2118, doi:10.1175/1520-0469(2003)060<2101:SSOTJ>2.0.CO;2.

——, and ——, 2007: Structure and spacing of jets in barotropic turbulence. *J. Atmos. Sci.,* **64,** 3652–3665, doi:10.1175/JAS4016.1.

Ferrari, R., and M. Nikurashin, 2010: Suppression of eddy diffusivity across jets in the Southern Ocean. *J. Phys. Oceanogr.,* **40,** 1501–1519, doi:10.1175/2010JPO4278.1.

Holloway, G., 2010: Eddy stress and shear in 2D flows. *J. Turbul.,* **11,** 1–14, doi:10.1080/14685248.2010.481673.

Kelvin, L., 1887: Stability of fluid motion: Rectilinear motion of viscous fluid between two parallel plates. *Philos. Mag.,* **24,** 188–196.

Klocker, A., R. Ferrari, and J. H. LaCasce, 2012: Estimating suppression of eddy mixing by mean flows. *J. Phys. Oceanogr.,* **42,** 1566–1576, doi:10.1175/JPO-D-11-0205.1.

Kraichnan, R. H., 1976: Eddy viscosity in two and three dimensions. *J. Atmos. Sci.,* **33,** 1521–1536, doi:10.1175/1520-0469(1976)033<1521:EVITAT>2.0.CO;2.

Li, L., A. P. Ingersoll, and X. Huang, 2006: Interaction of moist convection with zonal jets on Jupiter and Saturn. *Icarus,* **180,** 113–123, doi:10.1016/j.icarus.2005.08.016.

Maddison, J., and D. Marshall, 2013: The Eliassen–Palm flux tensor. *J. Fluid Mech.,* **729,** 69–102, doi:10.1017/jfm.2013.259.

Manfroi, A. J., and W. R. Young, 1999: Slow evolution of zonal jets on the beta-plane. *J. Atmos. Sci.,* **56,** 784–800, doi:10.1175/1520-0469(1999)056<0784:SEOZJO>2.0.CO;2.

Orr, W. M. F., 1907: The stability or instability of the steady motions of a perfect liquid and of a viscous liquid. Part I: A perfect liquid. *Proc. Roy. Ir. Acad.,* **27A,** 9–68.

Rosen, G., 1971: General solution for perturbed plane Couette flow. *Phys. Fluids,* **14,** 2767–2769, doi:10.1063/1.1693404.

Scott, R. K., and L. M. Polvani, 2007: Forced-dissipative shallow-water turbulence on the sphere and the atmospheric circulation of the giant planets. *J. Atmos. Sci.,* **64,** 3158–3176, doi:10.1175/JAS4003.1.

Shepherd, T. G., 1985: Time development of small disturbances to plane Couette flow. *J. Atmos. Sci.,* **42,** 1868–1871, doi:10.1175/1520-0469(1985)042<1868:TDOSDT>2.0.CO;2.

Showman, A. P., 2007: Numerical simulations of forced shallow-water turbulence: Effects of moist convection on large-scale circulation of Jupiter and Saturn. *J. Atmos. Sci.,* **64,** 3132–3157, doi:10.1175/JAS4007.1.

Smith, K. S., 2004: A local model for planetary atmospheres forced by small-scale convection. *J. Atmos. Sci.,* **61,** 1420–1433, doi:10.1175/1520-0469(2004)061<1420:ALMFPA>2.0.CO;2.

Srinivasan, K., and W. R. Young, 2012: Zonostrophic instability. *J. Atmos. Sci.,* **69,** 1633–1656, doi:10.1175/JAS-D-11-0200.1.

Stewart, R., and R. Thomson, 1977: Re-examination of vorticity transfer theory. *Proc. Roy. Soc. London,* **354A,** 1–8, doi:10.1098/rspa.1977.0053.

Thomson, R. E., and R. Stewart, 1977: The balance and redistribution of potential vorticity within the ocean. *Dyn. Atmos. Oceans,* **1,** 299–321, doi:10.1016/0377-0265(77)90019-7.

Tung, K. K., 1983: Initial-value problems for Rossby waves in a shear flow with critical level. *J. Fluid Mech.,* **133,** 443–469, doi:10.1017/S0022112083002001.

Vallis, G. K., and M. E. Maltrud, 1993: Generation of mean flow and jets on a beta plane and over topography. *J. Phys. Oceanogr.,* **23,** 1346–1362, doi:10.1175/1520-0485(1993)023<1346:GOMFAJ>2.0.CO;2.

Welander, P., 1973: Lateral friction in the oceans as an effect of potential vorticity mixing. *Geophys. Astrophys. Fluid Dyn.,* **5,** 173–189, doi:10.1080/03091927308236114.

Williams, G. P., 1978: Planetary circulations: 1. Barotropic representation of Jovian and terrestrial turbulence. *J. Atmos. Sci.,* **35,** 1399–1426, doi:10.1175/1520-0469(1978)035<1399:PCBROJ>2.0.CO;2.